Study of nanocomposites with carbon nanotubes and their tendency for carbon organization

C. G. Renda[1]*, C. de Oliveira[1], R. Bertholdo[1]
[1]Federal University of Alfenas, Institute of Science and Technology, Poços de Caldas, MG, Brazil

Abstract

The carbon derived from the thermal treatment of modified phenolic resins (PR) tends to organize into graphitic lamellae or turbostratic carbon and is commonly considered non-graphitizable. In this study, nanocomposites were synthesized with modified phenolic resin (Novolac) used as the matrix and oxidized multi-walled carbon nanotubes (NT_{ox}) in amounts ranging from 0.3 to 2.5 wt% as a filler. Thermal gravimetric analysis (TGA), Raman spectroscopy, powder X-ray diffraction (XRD), scanning electron microscopy (SEM) with field emission gun (FEG), and transmission electron microscopy (TEM) were performed. By TGA, the PR-2.5 wt% nanocomposite showed less thermal degradation and higher stability when compared to the pure matrix after heat treatment up to 1000 °C. Graphitic carbon organization analysis by Raman spectroscopy, XRD, SEM/FEG, and TEM micrographs showed that the PR-2.5 wt% nanocomposite is suitable for technological applications, involving a carbon graphitization tendency.

Keywords: nanocomposites, modified phenolic resin, carbon nanotubes, graphitization, organized carbon.

INTRODUCTION

Nanostructured composites present interesting properties for the industries, such as electrical conductivity, water treatment, mechanical resistance, thermal stability, and char yield content [1-6]. In this regard, carbon nanotubes (CNT) are used as fillers in reinforced polymer nanocomposites [7] and in graphitized CNT/carbon composites due to their mechanical properties [8-10], carbon matrix alignment inducing graphitization, tensile strength, and electrical conductivity [11]. The thermal conductivity of filler, combined with its quality of dispersion and the interface with the polymer, improves the thermal conductivity of the nanocomposite [12]. Polymeric nanocomposites added with CNT may be prepared using various methods and have shown increasing thermal stability, especially when CNT is oxidized, improving their dispersion into the matrices [13].

Among the polymers used in carbon nanocomposites, the phenolic resin has stood out for presenting dimensional and thermal stability, chemical resistance at high temperatures, and low cost compared to other thermoset polymers found on the market [12, 14]. Phenolic resins (PR) have a wide range of applications, such as in heat-shields for the aerospace industry [4], automotive parts [15], refractory binders [16], wood adhesives [17], and others due to their fire retardant and electromagnetic interference shielding [18], low flammability, low smoke emission levels under fire conditions, and good chemical resistance [19, 20]. The use of pure PR as an integral part of composites/nanocomposites depends on its type of preparation [21-23]. Properties such as reactivity, thermal behavior, and structure have been consistently studied as they are not yet entirely understood [24].

A previous study obtained a better graphitization tendency of Novolac resin using a 0.33 phenol (P) and formaldehyde (F) molar ratio in an acidic medium [25] instead of phenol (P) excess [26]. During pyrolysis, resin microstructural changes occur transforming the amorphous carbon [27, 28] into a potential graphitized material due to chemical modification caused by excess formaldehyde and experimental procedure [25]. In this study, nanocomposites were produced using PR (0.33 P/F molar ratio) as a matrix and several oxidized nanotubes (NT_{ox}) as fillers. The optimal CNT concentration into PR nanocomposites was analyzed, focusing on carbon organization at temperatures up to 1000 °C to induce graphitization for future applications.

MATERIALS AND METHODS

Materials and samples' preparation: phenol (99% purity, Proquímios, Brazil) and formaldehyde (36-38 wt% solution, Proquímios, Brazil) in an acidic medium (hydrochloric acid, Vetec, Brazil) were used to synthesize the PRs. MWCNT with 10-40 nm diameter and 5-20 μm length and 95% purity was obtained by CNT Co.; HNO_3 (Proquímios, 69-71% solution) for MWCNT oxidation and ethyl alcohol R.G.-A.C.S (99.5% purity, Synth, Brazil) for MWCNT washing and redispersion were used. As suggested in a previous study [25], this modified Novolac resin was synthesized in the laboratory with formaldehyde excess and in an acidic medium to improve its carbon graphitization tendency. As evaluated by Renda and Bertholdo [25], the PR reaction at 0.33 molar ratio occurred in two steps, with the methylene bridges at the -ortho and -para positions and crosslinking occurring at the same positions, giving mobility to the structure for graphitization.

CNT oxidation: MWCNTs (called CNT) were dispersed in HNO_3 and refluxed at 120 °C for 1 h [29]. After that, the

*https://orcid.org/0000-0001-9013-3808

solution containing CNTs was filtered to remove the HNO_3 excess by vacuum filtration using an Anodisc 47 (0.02 μm pore size, 47 mm diameter, CAT n° 6809-5002, Whatman). The remaining CNTs were removed from the membrane and dispersed with distilled water by an ultrasonic bath. The dispersion and filtration processes were repeated until a neutral pH was reached. Afterward, ethyl alcohol was used in the final dispersion. The final material was heated at 50 °C for 24 h, ground in an agate mortar, and named NT_{ox}. The NT_{ox} sample was stored in a desiccator until added to the resin.

PR preparation: phenol and formaldehyde at a 0.33 molar ratio were placed in a beaker for 30 min under magnetic stirring. 3.2 molar hydrochloric acid solution was added to this mixture (under constant stirring), equivalent to a 2:3 volume ratio of HCl:formaldehyde, to accelerate the reaction rate. The solution was stirred for an extra 90 min. After that, two phases were obtained and separated using a separating funnel. The upper solution was opaque and contained un-reacted reagents. The denser and colorless phase was the prepolymer found at the bottom of the beaker. The *in situ* polymerization method was used in some studies [25, 30]. The same method was applied to obtain the PR used as the matrix for all nanocomposites in this study.

Nanocomposites preparation: the prepolymer phase was mechanically stirred and heated at 70 °C. After 2.5 min, NT_{ox} powders were added to the prepolymer under mechanical stirring to form nanocomposites. Stirring was ceased after achieving enough viscosity to mold the samples (amounts shown in Table I). The samples were stored in a desiccator until characterization.

Table I - Samples with varying NT_{ox} concentrations.

Sample	Weight of phenol (g)	Weight of NT_{ox} (g)	NT_{ox}/phenol (%)
PR-0.3	2.025	0.006	0.27
PR-0.7	2.025	0.014	0.67
PR-1.3	2.025	0.027	1.34
PR-2.5	2.025	0.052	2.55

Materials characterization: a thermal analyzer (STA 449 F3 Jupiter, Netzsch) was used to investigate the thermal behavior of nanocomposites. About 10 mg mass for each sample and covered platinum crucibles were used. The temperature ranged between 30 and 1000 °C under 50 mL/min argon flux at a 10 °C/min heating rate. After 1000 °C, the samples were cooled down to room temperature. For the carbon samples from phenolic resins in a tube furnace, similar conditions were used for the thermal gravimetric analysis (TGA). X-ray diffraction (XRD) and Raman spectroscopy techniques evaluated the graphitization tendency. A diffractometer (Ultima IV, Rigaku) with CuKα radiation (λ=1.5406 Å) was used for XRD analyses of crushed samples. Results were collected at 2θ between 5° and 70° at 2 °/min. For diffractograms deconvolution, Origin

software was used to obtain the interlamellar distance (d_{002}), using Bragg equation [31]:

$$n\lambda = d_{002}.2.\sin\theta \qquad\qquad (A)$$

where n is an integer number, λ the incident radiation wavelength, d the interplanar distance between atomic planes, and θ the incidence angle in relation to a considered plane. Raman spectra of samples were collected using a spectrophotometer (Labran HR, Horiba Sci.) coupled to an optical microscope with a He-Ne laser (632.8 nm) and 17 μW incidence power at the 200-2000 cm^{-1} range. The morphological analysis of nanocomposites in powder form was performed by scanning electron microscopy (SEM), using a microscope (FEG XL, Philips) operating at 30 kV, and analytical transmission electron microscopy (TEM) with a microscope (Tecnai G^2 20S Twin LaB6, FEI) operating from 20 to 200 kV. For the analysis, the nanocomposites in the powder form were dried, suspended in ethanol for 30 min, glued with carbon tape, and covered with a thin gold film

RESULTS AND DISCUSSION

PR characterization. Thermal analysis of nanocomposites: Fig. 1 presents TGA curves and Table II data summarizes the thermal stability information. Weight loss up to 300 °C may be attributed to reagents excess, catalyst, and/or components with imperfect crosslinks or unreacted monomers, prepolymer components decomposition, and free molecules, or also water resulting from condensation reaction [32]. Weight loss continued between 300 and 600 °C, indicating the emission of gaseous components such as carbon dioxide, methane, phenol, carbon monoxide, xylenols, and cresols [25]. Degradation temperature onset also occurred at this range [33]. In the presence of sp^2 bonds, oxidation may start at temperatures as low as 250 °C up to about 600 °C [34]. The higher PR degradation point occurred close to 600 °C [35]. Over 650 °C, a carbon-like structure was formed due to dehydration [3]. Furthermore, from this point on, the range was almost linear, corroborating with these authors. Until 1000 °C, samples were already thermally stable with minimal mass loss. Samples with lower amounts of CNT (up to 1.3%) presented similar thermal behavior to pure PR. Considering the residual weight at 900 °C, the sample with 2.5% NT_{ox} presented a weight loss 9% lower than pure PR and 20% lower than PR-0.7. For PR-2.5, thermal behavior improved as weight loss decreased. Minor disruption may be caused by NT_{ox} on the PR structure during the crosslink. In a study [36] using simulation software, the authors reported that pyrolysis kinetics is higher than PR dehydration (caused by condensation, crosslinking, and cure reactions), including the break of polymer chains into shorter molecules. Therefore, the claim that CNT added as the filler has no effect on the pyrolysis process is unjustifiable. They suggested that further studies are needed to understand the reaction kinetics in the experimental 573 to 1173 K temperature range, with different starting structures. Thus, this study proposes to investigate some of these nanocomposite structure aspects.
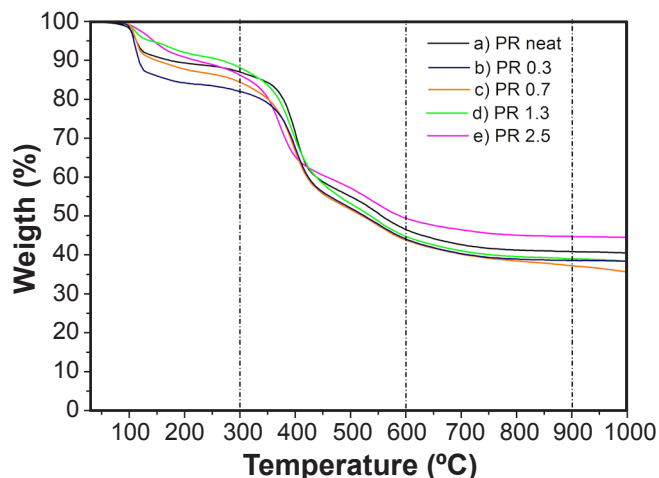
Figure 1: TGA analysis from nanocomposite samples.

Figure 2: XRD patterns for samples obtained after heat treatment (1000 °C).

Table II - Residual weight (%) at different temperatures for the nanocomposite samples.

Sample	300 °C	600 °C	900 °C	1000 °C
PR-neat	87	46	41	41
PR-0.3	82	44	39	38
PR-0.7	84	44	37	36
PR-1.3	88	45	39	38
PR-2.5	86	49	45	45

Analysis of nanocomposite graphitization tendencies: carbon samples obtained from nanocomposite pyrolysis were analyzed by XRD and Raman spectroscopy. In X-ray diffractograms, graphitic planes presented thin and intense peaks at 2θ ~26° (002) and ~44.5° (100). Non-graphitic planes presented wide peaks at ~24° and ~42° [37]. Fig. 2 shows X-ray diffractograms with a broad d_{002} characteristic peak, indicating the presence of disordered carbon. Data of this interplanar distance are seen in Table III. The interlamellar distance (d_{002}) for pure PR, PR-2.5, and graphite were 3.489, 3.378, and 3.354 Å, respectively. However, for different nanotextures (i.e. pyrolytic carbon and carbon fibers) using just the d_{002} value to obtain the graphitization level may pose a danger [38].

Fig. 3 shows Raman spectra with three major bands:

G-band around 1588 cm^{-1}, a graphitic carbon characteristic band; D'-band (around 1620 cm^{-1}), and D-band (around 1250-1400 cm^{-1}), both representing defect bands [39-41] added to compose I_D intensity. Table III shows the Raman results. The types of functional groups created (-OH, >C=O and -COOH) on the CNT walls depend on the treatment used for oxidation [29, 42], and they allow the CNT to interact with the resin and promote the synergistic effect. By using the proposed oxidation type, some defects created in NT_{ox} walls decreased the I_D/I_G ratio compared to CNT. CNT I_D/I_G ratio indicates the level of deterioration when oxidized [42]. This treatment was not so aggressive since adding NT_{ox} to PR for the PR-2.5 sample caused the I_D/I_G ratio to return to that value close to the initial CNT ratio. The I_D/I_G ratio for PR-2.5 was better than NT_{ox} and similar to CNT: CNT>PR-2.5>NT_{ox} (1.552>1.878>2.891) as seen in Table III. In this study, the I_D/I_G ratio for PR used as the matrix presented a 2.281 value. The result for PR-2.5 was improved, resulting from a synergistic effect with this NT_{ox} amount. Thus far, these techniques indicated that PR-2.5 is the best nanocomposite for carbon graphitization tendency, so its microstructure was investigated.

Nanocomposite microstructure analysis: Fig. 4 shows

Table III - XRD and Raman data of the nanocomposites.

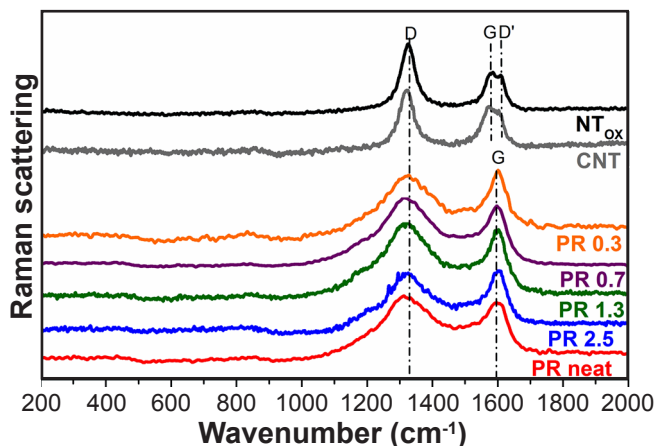| Sample	d_{002} (Å)	D position (cm^{-1})	D' position (cm^{-1})	G position (cm^{-1})	I_D/I_G
CNT	3.294	1321	1607	1574	1.552
NT_{ox}	3.202	1320	1603	1572	2.891
PR-neat	3.489	1327	-	1589	2.281
PR-0.3	3.267	1328	-	1599	2.088
PR-0.7	3.471	1325	-	1592	3.241
PR-1.3	3.448	1325	-	1595	2.994
PR-2.5	3.378	1329	-	1595	1.878

Figure 3: Raman spectra of samples after heat treatment (1000 °C).
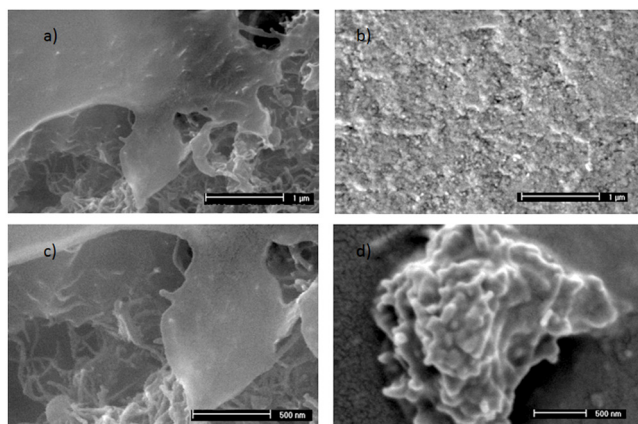

Figure 4: SEM images of nanocomposite PR-2.5 before (a,c) and after (b,d) heat treatment (1000 °C).
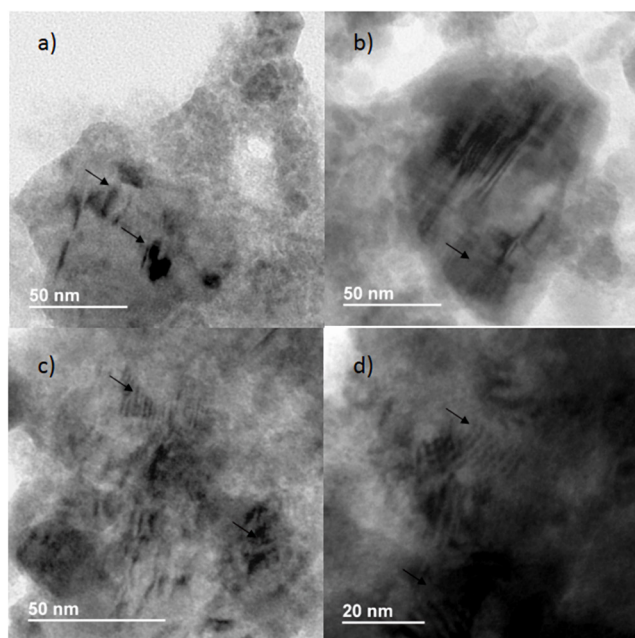

Figure 5: TEM images of PR-2.5 sample showing carbon graphitization tendency highlighted by arrows.

the SEM/FEG images of PR-2.5 nanocomposite at different magnifications. Microstructures before (Figs. 4a and 4c) and after heat treatment up to 1000 °C (Figs. 4b and 4d). Figs. 4a and 4c present NT_{ox} in lighter gray. Partial agglomeration occurred before thermal treatment, and the PR microstructure presented higher roughness after heat treatment (Figs. 4b and 4d).

TEM images of nanocomposites after heat treatment up to 1000 °C are shown in Figs. 5a to 5d at different magnifications. The dark striped regions were composed of organized carbons, highlighted with arrows. They represent either organized planes formation or their carbon graphitization tendency. Carbon organization during heat treatment starts with turbostratic structures or intermediary carbon organization, which have nearly parallel graphitic fragments regions above 1 nm ending in graphitic structures with perfectly aligned lamellae [25, 43]. The SEM and TEM images corroborated with previous analyses in this study and the previous study [25], highlighting organized regions. The nanocomposites presented three types of structures: turbostratic, graphitic, and amorphous. The synthesis method with PR-2.5 showed a higher graphitization tendency and therefore may be used in technological, thermal, and other applications.

CONCLUSIONS

Nanocomposites with varying CNT amounts were prepared and analyzed for their carbon graphitization tendency. The TGA results confirmed greater thermal stability of nanocomposite with 2.5% of oxidized nanotubes (NT_{ox}). XRD and Raman analyses of carbons obtained after up to 1000 °C heat treatment showed that PR-2.5 nanocomposite presented the smallest carbon structure defects and formed a graphitic nanostructure with some graphitization level. Phenolic resin chemical modification and the addition of 2.5 wt% CNT in relation to phenol generated a crosslinked structure sufficiently stable against oxidation. This characteristic avoided steric hindrance, providing malleability to lose the methylene bonds between the phenolic rings and obtaining the carbon turbostratic or graphitic lamellae when treated up to 1000 °C. These results were confirmed by some graphitization levels, as shown by SEM/TEM analyses. In conclusion, the nanocomposites prepared with 2.5% NT_{ox} and Novolac resin 0.33 molar ratio (P/F) may be qualified as potential material for applications in the technological area involving graphitized carbon.

ACKNOWLEDGEMENTS

REFERENCES

[1] C.L. Chiang, C.C.M. Ma, Polym. Degrad. Stab. **83** (2004) 207.

[2] S. Shahi, H. Roghani-Mamaqani, M. Salami-Kalajahi, H. Ebrahimi, Polym. Test. **68** (2018) 467.

[3] Z. Wang, D. Kwon, G. Gu, W. Lee, J. Park, K.L. DeVries, J. Park, Compos. B Eng. **60** (2014) 597.

[4] D.C. Wood, P.J. Hazell, G.J. Appleby-Thomas, N.R. Barnes, J. Mater. Sci. **46** (2011) 5991.

[5] M.A. Abd El-Ghaffar, A.M. Youssef, A.A. Abd El-Hakim, Arab. J. Chem. **8** (2015) 771.

[6] A.M. Youssef, F.M. Malhat, A.A. Abdel Hakim, I. Dekany, Arab. J. Chem. **10** (2017) 631.

[7] Z.G. Ayanoglu, M. Dogan, Diam. Relat. Mater. **108** (2020) 107950.

[8] P. Ma, N.A. Siddiqui, G. Marom, J. Kim, Compos. Part A Appl. Sci. Manuf. **41** (2010) 1345.

[9] L. Ma, R. Zhang, H. Niu, Z. Lu, Y. Huang, Diam. Relat. Mater. **112** (2021) 108250.

[10] H. Moustafa, N.A. Darwish, A.M. Youssef, J. Adhes. **97** (2021) 801.

[11] Y. Han, S. Li, F. Chen, T. Zhao, Mater. Today Commun. **6** (2016) 56.

[12] S. Zhao, J. Cui, G. Zhang, A. Gao, Y. Yan, Polym. Compos. **40**, 11 (2019) 4248.

[13] H. Ebrahimi, H. Roghani-Mamaqani, M. Salami-Kalajahi, S. Shahi, A. Abdollahi, Polym. Compos. **39** (2018) E1231.

[14] I. Hwang, C. Jung, I. Kuk, J. Choi, Y. Nho, Nucl. Instrum. Methods Phys. Res. B **268** (2010) 3386.

[15] K. Hirano, M. Asami, React. Funct. Polym. **73** (2013) 256.

[16] J. Zhang, G. Mei, Z. Xie, S. Zhao, ISIJ Int. **56**, 1 (2016) 44.

[17] S. Cheng, Z. Yuan, M. Anderson, M. Leitch, C. Xu, J. Appl. Polym. Sci. **126** (2012) E430.

[18] V.K. Patle, R. Kumar, A. Sharma, N. Dwivedi, D. Muchhala, A. Chaudhary, Y. Mehta, D.P. Mondal, A.K. Srivastava, Compos. C Open Acc. **2** (2020) 100020.

[19] H. Shen, A.J. Lavoie, S.R. Nutt, Compos. Part A Appl. Sci. Manuf. **34** (2003) 941.

[20] C.S. Bitencourt, V.C. Pandolfelli, Cerâmica **59**, 349 (2013) 1.

[21] G. Pulci, J. Tirillo, F. Marra, F. Fossati, C. Bartuli, T. Valente, Compos. Part A Appl. Sci. Manuf. **41** (2010) 1483.

[22] S. Lei, Q. Guo, D. Zhang, J. Shi, L. Liu, X. Wei, J. Appl. Polym. Sci. **117** (2010) 3345.

[23] H. Chen, M. Zhou, Z. Wang, S. Zhao, S. Guan, Electrochim. Acta **148** (2014) 187.

[24] Y. Zaks, J. Lo, D. Raucher, E.M. Pearce, J. Appl. Polym. Sci. **27** (1982) 913.

[25] C.G. Renda, R. Bertholdo, J. Polym. Res. **25**, 11 (2018) 241.

[26] B. Strzemiecka, J. Zieba-Palus, A. Voelkel, T. Lachowicz, E. Socha, J. Chromatogr. A **1441** (2016) 106.

[27] B. Rand, B. McEnaney, Br. Ceram. Trans. J. **84** (1985) 157.

[28] Y. Yamashita, K. Ouchi, Carbon **19** (1981) 89.

[29] K.A. Wepasnick, B.A. Smith, K.E. Schrote, H.K. Wilson, S.R. Diegelmann, D.H. Fairbrother, Carbon **49** (2011) 24.

[30] J. Cui, Y. Yan, J. Liu, Q. Wu, Polym. J. **40**, 11 (2008) 1067.

[31] M.B. Vázquez-Santos, E. Geissler, K. László, J. Rouzaud, A. Martínez-Alonso, J.M.D. Tascón, J. Phys. Chem. C **116** (2012) 257.

[32] R. Jones, G.M. Jenkins, Carbon **14** (1976) 292.

[33] M.R. Schutz, K. Sattler, S. Deeken, O. Klein, V. Adasch, C.H. Liebscher, U. Glarzel, J. Senker, J. Breu, J. Appl. Polym. Sci. **117** (2010) 2272.

[34] H.O. Pierson, *Handbook of carbon, graphite, diamond and fullerenes: properties, processing and applications*, Noyes Publ., New Jersey (1993).

[35] B. Roszek, W.H. de Jong, R.E. Geertsma, *Nanotechnology in medical applications: state-of-the-art in materials and devices*, Nat. Inst. Publ. Health Environ., Utrecht (2005).

[36] T.G. Desai, J.W. Lawson, P. Keblinski, Polymer **52** (2011) 577.

[37] C.S. Bitencourt, A.P. Luz, C. Pagliosa, V.C. Pandolfelli, Ceram. Int. **41**, 10 (2015) 13320.

[38] N. Iwashita, M. Inagaki, Carbon **31**, 7 (1993) 1107.

[39] A. Cuesta, P. Dhamelincourt, J. Laureyns, A. Martínez-Alonso, J.M.D. Tascón, Carbon **32**, 8 (1994) 1523.

[40] A. Cuesta, P. Dhamelincourt, J. Laureyns, A. Martínez-Alonso, J.M.D. Tascón, J. Mater. Chem. **8** (1998) 2875.

[41] L.G. Cançado, K. Talai, T. Enoki, Appl. Phys. Lett. **88** (2006) 163106.

[42] Z. Jia, Z. Wang, J. Liang, B. Wei, D. Wu, Carbon **37** (1999) 903.

[43] J. Zhang, J. Shi, Y. Zhao, Q. Guo, L. Liu, Z. Feng, Z. Fan, J. Mater. Sci. **47** (2012) 5891.